The 2010 IEEE/RSJ International Conference on
Intelligent Robots and Systems
October 18-22, 2010, Taipei, Taiwan

A Walking Pattern Generator for Biped Robots on Uneven Terrains

Yu Zheng, Ming C. Lin, Dinesh Manocha *
Albertus Hendrawan Adiwahono, Chee-Meng Chew †

Abstract

We present a new method to generate biped walking patterns for biped robots on uneven terrains. Our formulation uses a universal stability criterion that checks whether the resultant of the gravity wrench and the inertia wrench of a robot lies in the convex cone of the wrenches resulting from contacts between the robot and the environment. We present an algorithm to compute the feasible acceleration of the robot's CoM (center of mass) and use that algorithm to generate biped walking patterns. Our approach is more general and applicable to uneven terrains as compared with prior methods based on the ZMP (zero-moment point) criterion. We highlight its applications on some benchmarks.

1. Introduction

Biped walking is a key problem in the design of humanoid robots. One of the most successful stability criteria for walking robots is the ZMP criterion, which determines if the ZMP is inside the support polygon of the feet of a robot [1]. An in-depth review of the ZMP can be found in [2]. Based on the ZMP criterion, many methods to generate walking patterns have been proposed, such as [3]–[8]. However, the original ZMP criterion is primarily limited to cases where a robot walks on a horizontal flat terrain with sufficiently large friction. Several attempts have been made to extend these methods to handle terrains with slopes or stairs [9]–[12], but their applications have been limited.

Main results: We present a walking pattern generator for a biped robot to follow given foot placements on an arbitrary terrain, based on a general stability criterion [13] and an efficient way to verify it [14]. We develop algorithms to compute stable CoM positions with respect to foot placements and a trajectory such that the CoM moves from the initial position to the goal. The resulting generator tends to produce good trajectories for a robot to stably walk over several complex terrains.

The rest of this paper is organized as follows. Section 2 summarizes prior work. Section 3 is an overview of our generator. Section 4 formulates the general stability criterion. Sections 5 and 6 explain the details of our generator. Section 7 reports the simulation results. Section 8 concludes with possible future directions.

2. Related Work

The ZMP criterion is frequently used in generating walking patterns for biped robots. Some methods generate the body motion according to a pre-determined ZMP trajectory [3], [4]. Another set of methods utilize the ZMP criterion to verify the stability of a robot following a planned body trajectory [5]–[8]. Some researchers extended the ZMP criterion to more general cases, where robot's hands come into contact with the environment as well [9], [10] or a robot walks on rough terrains [11] or slopes and stairs [12].

In order to overcome the limitations, a general stability criterion has been suggested instead of the ZMP criterion, which determines if the gravity [15] or the resultant of the gravity and the inertia wrench [13], [16] lies in the convex cone of feasible wrenches from contacts between a robot and its environment. Hauser *et al.* [17] used the static stability criterion [15] in designing a motion planner for legged robots walking on rough terrains. However, there is relatively little work on walking pattern generation based on a general dynamic stability criterion [13], [16]. One main reason is that verifying the dynamic stability of a biped robot is much more complex than the static stability or the ZMP.

*Y. Zheng, M. C. Lin, and D. Manocha are with the Department of Computer Science, University of North Carolina at Chapel Hill, NC 27599 USA {yuzheng,lin,dm}@cs.unc.edu. This work was supported by ARO Contract W911NF-04-1-0088, NSF awards 0636208, 0917040 and 0904990, DARPA/RDECOM Contract WR91CRB-08-C-0137, and Intel.

†A. H. Adiwahono and C.-M. Chew are with the Department of Mechanical Engineering, National University of Singapore, Singapore 117576 {albertus,chewcm}@nus.edu.sg.

Algorithm 1. Generate the walking pattern for a task

Input: initial and goal configurations of a robot; a sequence of foot placements on the ground.
Output: trajectories of the CoM and all joints such that the robot walks to the goal along foot placements.

```
Adjust the robot (a typical motion is to squat down)
repeat
    Compute the position of the CoM supported by only one foot such that the other foot can lift up and shift to its next placement
    Move the CoM from the current position to the position computed above, while both feet still remain on the ground; calculate the joint angles on both legs using inverse kinematics
    Shift the swing leg to its next placement, while holding the CoM to its current position
until both feet reach their final placements
Adjust the robot to the goal configuration
```

3. Overview

Given foot placements on the ground that can be pre-determined by footstep planning algorithms [18]–[20], our objective is to compute a stable CoM trajectory and joint angles of each leg such that the robot walks, following those foot placements.

In this paper, we consider a biped robot walking on uneven terrains, on which the robot's feet may have different orientations at every step and the normals at contacts on both feet are not parallel. In such cases, maintaining the robot's stability is much more difficult than on a flat horizontal terrain. To do this, we adopt an intermittent walking strategy; that is, the CoM of the robot stays in a certain position when a leg swings and it moves when both feet remain on the ground. Unlike walking on a flat horizontal terrain, where the CoM usually moves along with the swing leg without pause, alternately moving the CoM and a foot may limit the walking speed and scope of a robot. However, this facilitates the maintenance of the robot's stability on uneven terrains. Before the swing foot lifts up, we require the CoM to reach a certain position, in which the robot can maintain its stability with the support of only the other foot. When the CoM changes, both feet provide maximum support such that a stable trajectory of the CoM can be more easily computed. The walking circle is described in **Algorithm 1**.

4. Wrenches and Stability

In this section, we introduce a general stability criterion in terms of wrenches applied to a robot.

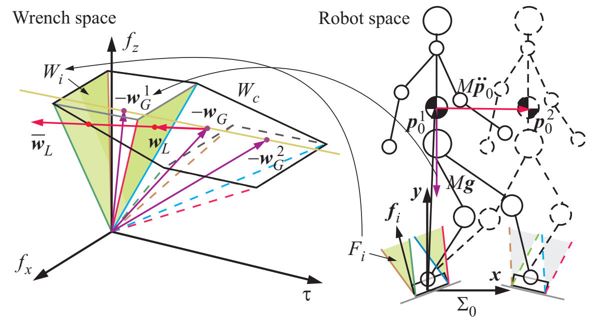

Fig. 1. View of biped walking in wrench space. The friction cone F_i, the gravity force $\boldsymbol{Mg}$, and the linear inertia force $M\ddot{\boldsymbol{p}}_0$ in robot space are transformed into the convex cone W_i, the gravity wrench $\boldsymbol{w}_G$, and the linear inertia wrench $\boldsymbol{w}_L$ in wrench space, respectively. The Minkowski sum of W_i for all contacts generates a convex cone W_c, which comprises all feasible wrenches that can be applied to the robot from contacts. As the position $\boldsymbol{p}_0$ of the CoM moves from $\boldsymbol{p}_0^1$ to $\boldsymbol{p}_0^2$, $-\boldsymbol{w}_G$ moves from $-\boldsymbol{w}_G^1$ to $-\boldsymbol{w}_G^2$. We keep $-\boldsymbol{w}_G + \boldsymbol{w}_L \in W_c$ in the interior of W_c such that there is enough stability margin to contain the angular inertia wrench $\boldsymbol{w}_A$, i.e., $-\boldsymbol{w}_G + \boldsymbol{w}_L + \boldsymbol{w}_A \in W_c$.

4.1. Wrenches (Forces and Moments)

Fig. 1 shows a biped robot. All contacts between the robot and the environment are assumed to be hard point contacts with friction. The bottom of each foot is flat, so that the contact normal is perpendicular to the foot. If a foot makes a planar contact with the environment, the planar contact can be treated as a few point contacts on its boundary. Let Σ_0 be the global coordinate frame whose z-axis is vertical. We decompose the wrenches exerted on the robot into four categories.

4.1.1. Contact wrench. The resultant wrench from all contacts with respect to the frame Σ_0 can be written as

$$\boldsymbol{w}_C = \sum_{i=1}^{m} \begin{bmatrix} \boldsymbol{I}_{3\times3} \\ \boldsymbol{r}_i \otimes \end{bmatrix} \boldsymbol{f}_i \tag{1}$$

where $\boldsymbol{r}_i$ denotes the position vector of a contact point between the robot and the environment in the frame Σ_0, $\boldsymbol{f}_i$ is the contact force, and $\boldsymbol{I}_{3\times3}$ is the 3×3 identity matrix. To avoid slip at contact, $\boldsymbol{f}_i$ must comply with the Coulomb friction constraint, which limits $\boldsymbol{f}_i$ into a convex cone F_i specified by

$$F_i = \{\boldsymbol{f}_i \in \mathbb{R}^3 | \parallel (\boldsymbol{I}_{3\times3} - \boldsymbol{n}_i\boldsymbol{n}_i^T)\boldsymbol{f}_i \parallel \leq \mu \boldsymbol{n}_i^T \boldsymbol{f}_i\} \tag{2}$$

where $\boldsymbol{n}_i$ is the unit normal at contact and μ is the Coulomb friction coefficient. Let W_i be the set of wrenches that can be generated by forces at contact i satisfying (2); i.e., $W_i = \{\begin{bmatrix}\boldsymbol{f}_i^T & (\boldsymbol{r}_i \otimes \boldsymbol{f}_i)^T\end{bmatrix}^T | \boldsymbol{f}_i \in F_i\}$. Let $W_c = \sum_{i=1}^{m} W_i$, which consists of all $\boldsymbol{w}_C$ given by (1) with $\boldsymbol{f}_i \in F_i$, $i = 1, 2, \ldots, m$ and is the set of all feasible resultant wrenches from contacts. It turns out that both W_i and W_c are convex cones.

4.1.2. Gravity wrench. The gravity and the resulting moment with respect to the origin of Σ_0 are given by

$$\boldsymbol{w}_G = \begin{bmatrix} \boldsymbol{I}_{3\times 3} \\ \boldsymbol{p}_0 \otimes \end{bmatrix} M\boldsymbol{g} \tag{3}$$

where $\boldsymbol{p}_0$ is the position of the CoM in Σ_0, M is the total mass of the robot, and $\boldsymbol{g} = \begin{bmatrix} 0 & 0 & -g \end{bmatrix}^T$. The wrench $\boldsymbol{w}_G$ is related only to the position $\boldsymbol{p}_0$ of the CoM.

4.1.3. Linear inertia wrench. It is the wrench generated by the inertia force applied to the CoM:

$$\boldsymbol{w}_L = \begin{bmatrix} \boldsymbol{I}_{3\times 3} \\ \boldsymbol{p}_0 \otimes \end{bmatrix} M\ddot{\boldsymbol{p}}_0 \tag{4}$$

where $\ddot{\boldsymbol{p}}_0$ is the acceleration of the CoM. The wrench $\boldsymbol{w}_L$ depends on $\boldsymbol{p}_0$ and $\ddot{\boldsymbol{p}}_0$. For a given $\boldsymbol{p}_0$, the direction of $\boldsymbol{w}_L$ is determined by the direction of $\ddot{\boldsymbol{p}}_0$, while their magnitudes are proportional to each other.

4.1.4. Angular inertia wrench. According to [13], the angular inertia wrench can be computed by

$$\boldsymbol{w}_A = \begin{bmatrix} \boldsymbol{0} \\ \dot{\boldsymbol{L}} \end{bmatrix} \tag{5}$$

where $\boldsymbol{L}$ is the angular momentum of the robot with respect to the CoM [13]:

$$\boldsymbol{L} = \sum_{j=1}^{N} \{ m_j (\boldsymbol{p}_j - \boldsymbol{p}_0) \otimes \dot{\boldsymbol{p}}_j + \boldsymbol{I}_j \boldsymbol{\omega}_j \} \tag{6}$$

where m_j, $\boldsymbol{p}_j$, $\boldsymbol{I}_j$, and $\boldsymbol{\omega}_j$ are the mass, position, inertia tensor, and angular velocity of the j-th link of the robot, respectively.

4.2. Stability criterion

A robot is *statically stable* if its gravity wrench can be counter-balanced by some contact forces; i.e., there exists $\boldsymbol{w}_C \in W_c$ such that $\boldsymbol{w}_C + \boldsymbol{w}_G = \boldsymbol{0}$, or equivalently $-\boldsymbol{w}_G \in W_c$. The *dynamic stability* also takes the inertia wrenches $\boldsymbol{w}_L$ and $\boldsymbol{w}_A$ into account and requires $\boldsymbol{w}_C + \boldsymbol{w}_G - \boldsymbol{w}_L - \boldsymbol{w}_A = \boldsymbol{0}$ for some $\boldsymbol{w}_C \in W_c$, which is equivalent to $-\boldsymbol{w}_G + \boldsymbol{w}_L + \boldsymbol{w}_A \in W_c$. Normally, we require $-\boldsymbol{w}_G$ or $-\boldsymbol{w}_G + \boldsymbol{w}_L + \boldsymbol{w}_A$ to be inside the interior of W_c such that there is some safety margin.

The formulation of W_c by (1) and (2) considers the contact normal $\boldsymbol{n}_i$ and the friction coefficient μ in general, unlike the ZMP criterion which assumes all contact normals to be vertical and the friction coefficient to be sufficient. Hence, the stability criterion based on W_c is generally applicable.

5. Statically Stable CoM Position

Here, given the contact positions of one single foot on the ground, we determine the position of the CoM such that the robot achieves static stability in that position or $-\boldsymbol{w}_G \in W_c$. Here W_c is generated with respect to the single supporting foot. We assume that the CoM is at a constant height h. Then $\boldsymbol{p}_0$ can be written as

$$\boldsymbol{p}_0 = \bar{\boldsymbol{p}}_0 + \rho(\cos\theta \boldsymbol{b}_1 + \sin\theta \boldsymbol{b}_2) \tag{7}$$

where $\bar{\boldsymbol{p}}_0$ is an arbitrary point in the horizontal plane at height h, and $\boldsymbol{b}_1$ and $\boldsymbol{b}_2$ are two unit orthogonal vectors that span the plane, and $\rho \geq 0$ and $\theta \in [0, 2\pi)$ are two scalar variables. We simply choose $\bar{\boldsymbol{p}}_0 = \begin{bmatrix} 0 & 0 & h \end{bmatrix}^T$, $\boldsymbol{b}_1 = \begin{bmatrix} 1 & 0 & 0 \end{bmatrix}^T$, and $\boldsymbol{b}_2 = \begin{bmatrix} 0 & 1 & 0 \end{bmatrix}^T$, and discretize θ as $\theta_k = 2k\pi/K$, $k = 0, 2, \ldots, K-1$; thus the problem is reduced to determining the domain of ρ such that $-\boldsymbol{w}_G \in W_c$. Substituting (7) into (3) yields

$$\begin{aligned} \boldsymbol{w}_G &= \begin{bmatrix} \boldsymbol{I}_{3\times 3} \\ \bar{\boldsymbol{p}}_0 \otimes \end{bmatrix} M\boldsymbol{g} + \rho \begin{bmatrix} \boldsymbol{0} \\ (\cos\theta_k \boldsymbol{b}_1 + \sin\theta_k \boldsymbol{b}_2) \otimes M\boldsymbol{g} \end{bmatrix} \\ &= \bar{\boldsymbol{w}}_G + \rho \boldsymbol{w}_k. \end{aligned}$$

The above equation means that $-\boldsymbol{w}_G$ lies on the ray originating from $-\bar{\boldsymbol{w}}_G$ in the direction $-\boldsymbol{w}_k$. The intersections of the boundary of W_c with the ray give the lower and upper bounds of ρ, denoted by ρ_k^{L} and ρ_k^{U}, such that $-\boldsymbol{w}_G \in W_c$. Substituting ρ_k^{L} and ρ_k^{U} together with θ_k into (7) leads to two points, between which any point gives a statically stable position of the CoM. By doing this for all $k = 0, 1, \ldots, K-1$, we obtain a set of points and observe: *1) the statically stable domain of the CoM is the convex hull of these points and 2) the shape of the domain or the x- and y-coordinates of these points are independent of the height h.*

We choose the CoM position with respect to the single supporting foot in **Algorithm 1** (line 3) at the center of the computed stable domain. Hence, the robot can possess a large stability margin.

6. Dynamically Stable CoM Trajectory

Let $\boldsymbol{p}_0^1$ and $\boldsymbol{p}_0^2$ be the current and next positions of the CoM computed by the above means with respect to two adjacent foot placements. Now we introduce an algorithm to generate a trajectory of the CoM from $\boldsymbol{p}_0^1$ to $\boldsymbol{p}_0^2$, which satisfies the dynamic stability criterion. According to the adopted walking strategy, the velocity of the CoM at $\boldsymbol{p}_0^1$ and $\boldsymbol{p}_0^2$ is zero and both feet keep touching the ground while the CoM moves from $\boldsymbol{p}_0^1$ towards $\boldsymbol{p}_0^2$. Thus, W_c here is generated with respect to two feet, different from that in Section 5.

In computing the trajectory of the CoM, we first omit $\boldsymbol{w}_A$. Then the dynamic stability criterion is simplified to $-\boldsymbol{w}_G + \boldsymbol{w}_L \in W_c$. Let $\boldsymbol{a}$ and λ be the direction and magnitude of $\ddot{\boldsymbol{p}}_0$, i.e., $\ddot{\boldsymbol{p}}_0 = \lambda \boldsymbol{a}$, where $\| \boldsymbol{a} \| = 1$ and $\lambda \geq 0$. From (4), for given $\boldsymbol{p}_0$ and $\ddot{\boldsymbol{p}}_0$, $\boldsymbol{w}_L = \lambda \begin{bmatrix} \boldsymbol{I}_{3\times3} \\ \boldsymbol{p}_{0\otimes} \end{bmatrix} M\boldsymbol{a} = \lambda \bar{\boldsymbol{w}}_L$, where $\bar{\boldsymbol{w}}_L = \begin{bmatrix} \boldsymbol{I}_{3\times3} \\ \boldsymbol{p}_{0\otimes} \end{bmatrix} M\boldsymbol{a}$. This implies that $-\boldsymbol{w}_G + \boldsymbol{w}_L = -\boldsymbol{w}_G + \lambda \bar{\boldsymbol{w}}_L$ is a point on the ray originating from $-\boldsymbol{w}_G$ in the direction $\bar{\boldsymbol{w}}_L$ for any $\lambda \geq 0$. The robot can accelerate in the direction $\boldsymbol{a}$ only if the ray intersects W_c. An efficient way to determine if a ray intersects a convex cone can be found at http://gamma.cs.unc.edu/RobotWalk/.

Since the CoM has no initial velocity and is required to move from $\boldsymbol{p}_0^1$ to $\boldsymbol{p}_0^2$, we choose $\boldsymbol{a} = (\boldsymbol{p}_0^2 - \boldsymbol{p}_0^1)/ \| \boldsymbol{p}_0^2 - \boldsymbol{p}_0^1 \|$. To determine an appropriate magnitude of acceleration, we need to compute the closest and farthest intersection points of W_c with the above ray, which represent the minimum and maximum magnitudes of feasible acceleration in that direction, namely $\lambda_{\min}$ and $\lambda_{\max}$. Then the acceleration magnitude can be calculated by $\lambda = (1-k)\lambda_{\min} + k\lambda_{\max}$, where $0 \leq k \leq 1$. Here we choose a smaller k to ensure that $-\boldsymbol{w}_G + \boldsymbol{w}_L$ lies deeply in the interior of W_c and leave a larger stability margin so that $-\boldsymbol{w}_G + \boldsymbol{w}_L + \boldsymbol{w}_A \in W_c$ eventually. Once the acceleration, including both $\boldsymbol{a}$ and λ, is determined, the status of the robot's CoM is updated by

$$\dot{\boldsymbol{p}}_0(t+T) = \dot{\boldsymbol{p}}_0(t) + \ddot{\boldsymbol{p}}_0(t)T \tag{8}$$

$$\boldsymbol{p}_0(t+T) = \boldsymbol{p}_0(t) + \dot{\boldsymbol{p}}_0(t)T + \ddot{\boldsymbol{p}}_0(t)T^2/2 \tag{9}$$

where T is the time step.

From the new status of the CoM and the positions of the feet, the new joint angles as well as the positions $\boldsymbol{p}_j$ and the angular velocities $\boldsymbol{\omega}_j$ of the links of the robot's legs can be calculated using inverse kinematics. Thus, we can obtain the angular inertia wrench $\boldsymbol{w}_A$ and verify the entire dynamic stability criterion $-\boldsymbol{w}_G + \boldsymbol{w}_L + \boldsymbol{w}_A \in W_c$. The update is valid if this criterion is satisfied. If not so, we choose a smaller k to reduce the acceleration of the CoM so that the inertia wrenches $\boldsymbol{w}_L$ and $\boldsymbol{w}_A$ can be smaller. By doing this, we attain the walking pattern for one time step.

We also need to determine the timing to decelerate the robot such that the CoM can stop at the desired position $\boldsymbol{p}_0^2$. To do this, we try to decrease $\dot{\boldsymbol{p}}_0$ to zero from the newly updated position $\boldsymbol{p}_0$ and compare the final position $\boldsymbol{p}_0$ of the CoM with $\boldsymbol{p}_0^2$. If $\dot{\boldsymbol{p}}_0$ can be reduced to zero and the final $\boldsymbol{p}_0$ does not exceed $\boldsymbol{p}_0^2$, then we can continue to accelerate the robot and update its status as above; otherwise, if the final $\boldsymbol{p}_0$ exceeds $\boldsymbol{p}_0^2$, from then on we keep decelerating the robot until it reaches $\boldsymbol{p}_0^2$. To reduce $\dot{\boldsymbol{p}}_0$ and decelerate the robot, we perform the above acceleration computation along the direction $-\boldsymbol{a}$, which is opposite to $\dot{\boldsymbol{p}}_0$. By this means, we obtain the walking pattern for one step. Then, repeating this process for all foot placements will generate a complete walking pattern for the robot.

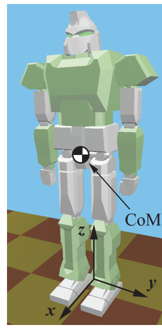

	Parameters		Joints	
	Mass (kg)	Length (mm)	Neck	pitch, yaw
Head	4	220	Shoulder	pitch, roll, yaw
Trunk	24	580	Elbow	pitch
Upper arm	3.5	320	Wrist	pitch, roll
Lower arm	2	280	Waist	roll, yaw
Hand	1.8	160	Hip	pitch, roll, yaw
Thigh	8	420	Knee	pitch
Shank	6	420	Ankle	pitch, roll
Foot	2.2	310 (Height 110)	Toe	pitch

Fig. 2. Parameters of the simulated robot.

7. Simulations

7.1. Simulation Setup

We conduct simulations in Webots. The simulated robot is about 1.75 m high and its CoM is at the hip and 0.84 m high when the robot stands upright. Fig. 2 exhibits the detailed parameters of the robot. The friction coefficient between the robot's feet and the ground is taken to be 0.5.

First, we let the robot walk over two sets of connected slopes with different inclination angles. The parameters of the slopes are listed in Table 1. Next, we have the robot walk over 12 different cylinders (Fig. 4), which are placed on the ground along a circle with a sweep angle of 60°. Table 2 displays their parameters. The upper surfaces of the cylinders are slopes and face along the (inward or outward) normal or the (forward or backward) tangent of the circle.

TABLE 1. PARAMETERS OF SLOPES

First slope set					
Inclination angles	20°	−10°	10°	−15°	−5°
Slope lengths (mm)	350	400	400	350	334
Second slope set					
Inclination angles	15°	−10°	20°	−15°	−10°
Slope lengths (mm)	450	400	400	400	462

7.2. Simulation Results

On the two slope sets, we keep the height of the robot's CoM at 0.72 m and 0.75 m, respectively. Fig. 3(a) and (b) shows the CoM trajectories generated by

TABLE 2. PARAMETERS OF CYLINDERS

Cylinders on the right side						
Inclination angles	5°	10°	20°	5°	15°	5°
Central heights (mm)	50	150	250	300	200	100
Cylinders on the left side						
Inclination angles	15°	10°	10°	10°	20°	5°
Central heights (mm)	100	200	300	250	150	50

Fig. 4. Snapshots of the simulated walk over cylinders.

our approach and the ones recorded in the simulation. The robot walking over the slopes is displayed in the accompanying video, which can be found at http://gamma.cs.unc.edu/RobotWalk/.

For the cylinder case, we allow the height of the robot's CoM to vary according to the heights of cylinders. The robot walking is exhibited with snapshots in Fig. 4 and the accompanying video on the above website. The CoM trajectory is plotted in Fig. 3(c). Finally the robot walks over the cylinders and turns 60°.

7.3. Discussion

In Fig. 3 it is observed that the CoM in the simulation (solid line) does not exactly follows the planned trajectory (dashed line). The reason is that we treat the CoM as a fixed point at the hip of the robot in planning its trajectory, while the leg swing can actually cause the CoM to deviate from that position. As shown in Fig. 3(a) and (b), the solid line starts to deviate from the dashed line where the dashed line becomes horizontal. That is the moment when one leg starts to swing. The deviation is relatively larger in the frontal plane, so that the difference in the y-coordinate of the CoM trajectory is more evident. Nevertheless, during the planning stage, we require the CoM to reach a position where $-\boldsymbol{w}_G$ is deeply inside W_c such that the robot achieves a large stability margin. Hence, after every deviation occurs, the robot can recover from it and continue to follow the planned trajectory. Furthermore, if the step length is not large, the deviation could be very small, as in the test of walking on cylinders (Fig. 3(c)).

8. Conclusion and Future Work

Based on a general stability criterion [13] and an efficient algorithm to verify it [14], we present a new approach to generating stable walking patterns for biped robots on uneven terrains. Its usefulness is demonstrated with simulations, where a humanoid robot walks over terrains with varying slopes. We would like to carry out more experiments on uneven or rough terrains to test our walking pattern generator. Further investigation may also consider the integration of this walking pattern generator with efficient collision detection and fast motion planning algorithms to build a complete system for biped locomotion in complex environments.

References

[1] M. Vukobratović and J. Stepanenko, "On the stability of anthropomorphic systems," *Mathematical Biosciences*, vol. 15 pp. 1–37, 1972.

[2] M. Vukobratović and B. Borovac, "Zero-moment point: thirty five years of its life," *International Journal of Humanoid Robotics*, vol. 1, No. 1, pp. 157-173, 2004.

[3] S. Kajita, F. Kanehiro, K. Kaneko, K. Fujiwara, K. Harada, K. Yokoi, H. Hirukawa, "Biped walking pattern generation by using preview control of zero-moment point," in *Proc. IEEE Int. Conf. Robot. Automat.*, Taipei, Taiwan, Sept. 2003, pp. 1620–1626.

[4] J. Park and Y. Youm, "General ZMP preview control for bipedal walking," in *Proc. IEEE Int. Conf. Robot. Automat.*, Roma, Italy, April 2007, pp. 2682–2687.

[5] Q. Huang, K. Yokoi, S. Kajita, K. Kaneko, H. Arai, N. Koyachi, K. Tanie, "Planning walking patterns for a biped robot," *IEEE Trans. Robot. Automat.*, vol. 17, no. 3, pp. 280–289, 2001.

[6] J. Kuffner, S. Kagami, K. Nishiwaki, M. Inaba, and H. Inoue, "Dynamically-stable motion planning for humanoid robots," *Autonomous Robots*, vol. 12, no.1, pp. 105–118, 2002.

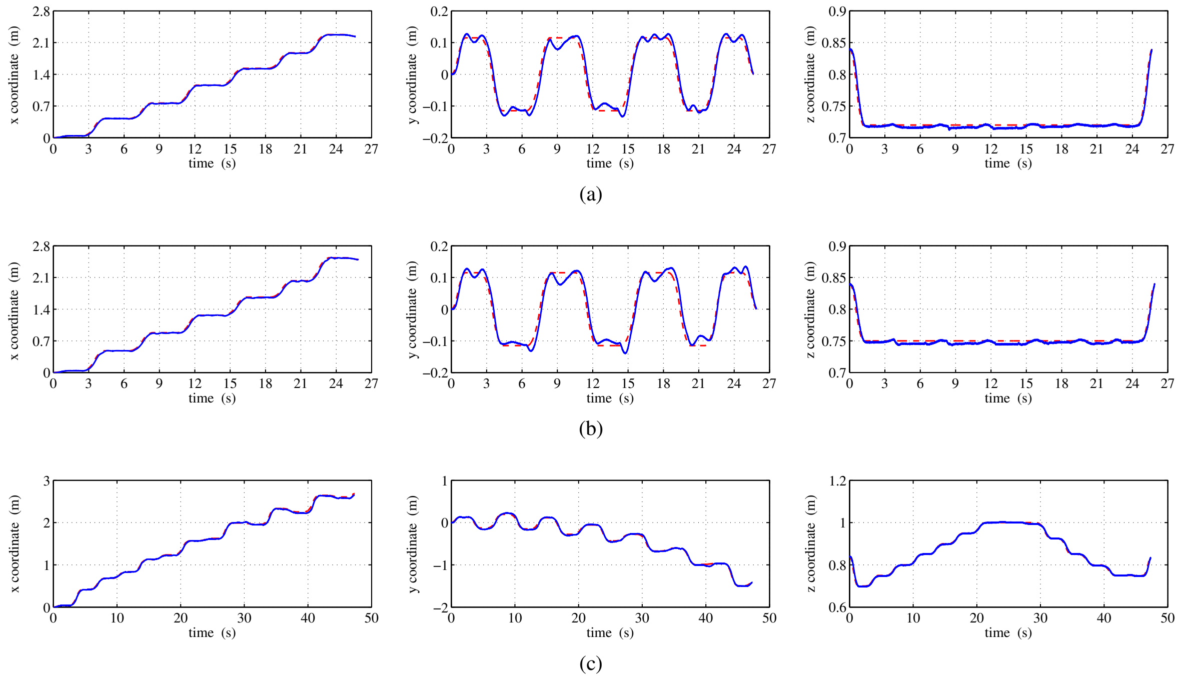

Fig. 3. The trajectories of the CoM on the (a) first slope set, (b) second slope set, and (c) cylinders. The dashed line represents the trajectory of the CoM generated by our method, while the solid line represents the one recorded in the simulation.

[7] E. S. Neo, K. Yokoi, S. Kajita, and K. Tanie, "Whole-body motion generation integrating operator's intention and robot's autonomy in controlling humanoid robots," *IEEE Trans. Robot.*, vol. 23, no. 4, pp. 763–775, 2007.

[8] F. Kanehiro, W. Suleiman, F. Lamiraux, E. Yoshida, and J.-P. Laumond, "Integrating dynamics into motion planning for humanoid robots," in *Proc. IEEE/RSJ Int. Conf. Intell. Robots Syst.*, Nice, France, Sept. 2008, pp. 660–667.

[9] S. Kagami, T. Kitagawa, K. Nishiwaki, T. Sugihiara, M. Inaba, and H. Inoue, "A fast dynamically equilibrated walking trajectory generation method of humanoid robot," *Auton. Robot.*, vol. 12, no.1, pp. 71–82, 2002.

[10] K. Harada, S. Kajita, K. Kaneko, and H. Hirukawa, "ZMP analysis for arm/leg coordination," in *Proc. IEEE/RSJ Int. Conf. Intell. Robots Syst.*, Las Vegas, Nevada, Oct. 2003, pp. 75–81.

[11] T. Sugihara, Y. Nakamura, and H. Inoue, "Realtime humanoid motion generation through ZMP manipulation based on inverted pendulum control," in *Proc. IEEE Int. Conf. Robot. Automat.*, Washington, DC, May 2002, pp. 1404–1409.

[12] W.-W. Huang, C.-M. Chew, Y. Zheng, and G.-S. Hong, "Pattern generation for bipedal walking on slopes and stairs," in *Proc. IEEE/RAS Int. Conf. Humanoid Robots*, Daejeon, Korea, Dec. 2008, pp. 205–210.

[13] H. Hirukawa, S. Hattori, K. Harada, S. Kajita, K. Kaneko, F. Kanehiro, K. Fujiwara, and M. Morisawa, "A universal stability criterion of the foot contact of legged robots - Adios ZMP," in *Proc. IEEE Int. Conf. Robot. Automat.*, Orlando, Florida, May 2006, pp. 1976–1983.

[14] Y. Zheng and C.-M. Chew, "Distance between a point and a convex cone in *n*-dimensional space: computation and applications," *IEEE Trans. Robot.*, vol. 25, no. 6, pp. 1397–1412, 2009.

[15] T. Bretl and S. Lall, "Testing static equilibrium for legged robots," *IEEE Trans. Robot.*, vol. 24, no. 4, pp. 794–807, 2008.

[16] T. Saida, Y. Yokokoji, and T. Yoshikawa, "FSW (feasible solution of wrench) for multi-legged robots," in *Proc. IEEE Int. Conf. Robot. Automat.*, Taipei, Taiwan, Sept. 2003, pp. 3815–3820.

[17] K. Hauser, T. Bretl, J.-C. Latombe, K. Harada, and B. Wilcox, "Motion planning for legged robots on varied terrain," *Int. J. Robot.Res.*, vol. 27, no. 11-12, pp. 1325–1349, 2008.

[18] J. Kuffner, K. Nishiwaki, S. Kagami, M. Inaba, and H. Inoue, "Footstep planning among obstacles for biped robots," in *Proc. IEEE/RSJ Int. Conf. Intell. Robot. Sys.*, Maui, HI, Oct. 2001, pp. 500–505.

[19] J. Kuffner, S. Kagami, K. Nishiwaki, M. Inaba, and H. Inoue, "Online footstep planning for humanoid robots," in *Proc. IEEE Int. Conf. Robot. Automat.*, Taipei, Taiwan, Sept. 2003, pp. 932–937.

[20] J. Chestnutt, J. Kuffner, K. Nishiwaki, and S. Kagami, "Planning biped navigation strategies in complex environments," in *Proc. IEEE Int. Conf. Humanoid Robots*, 2003.